Neural Network for Evaluating the Operational Range of Antennas with Randomly Generated Designs

Bartosz Czaplewski [1][0000-0001-7904-5567]

[1] Department of Teleinformation Networks, Faculty of Electronics, Telecommunications and Informatics, Gdansk University of Technology, Narutowicza 11/12, 80-233 Gdansk, Poland
bartosz.czaplewski@pg.edu.pl

Abstract. This paper introduces a novel machine learning-based methodology to determine the operational range of planar microstrip antennas of randomly generated designs, removing the need for electromagnetic (EM) simulations or expert knowledge. Framed as a multi-label classification task, the proposed approach addresses the inefficiencies of traditional methods, which are prone to high computational cost and engineer's bias. The method quickly identifies promising designs, paving the way for subsequent optimization. This advancement represents a significant step toward automating antenna design processes.

Keywords: Machine Learning, Neural Networks, Planar Microstrip Antennas

1 Introduction

Machine learning (ML) techniques have been widely used in communications, including antenna selection, malicious event detection, and mobility prediction. Applications such as SVM-based speech recognition and context-aware Internet of Things (IoT) show their flexibility. Deep learning has also impacted UAVs [1], THz communication [2], Wi-Fi [3], GPS [4], satellites [5], and IoT [6,7].

Antennas are essential for efficient signal transmission. Traditional design involves manual, iterative steps—substrate selection, shape definition, and parametric tuning—which are time-consuming, suboptimal, and prone to human bias. Automated, specification-driven methods use optimization algorithms [8–11] to improve designs but face challenges like geometry selection, dimensionality, and computation cost.

Automatically generated antennas follow two main models: compositions of basic shapes (e.g., rectangles or triangles) [12,13] and coordinate-based representations (e.g., splines or line segments) [14–16]. This work focuses on the latter, which allows flexibility but introduces issues: self-intersecting shapes, initializing geometry, and high dimensionality. Metaheuristics [16,17] partially address these but remain limited by electromagnetic (EM) simulation costs.

With no exact formulae for antenna topology, initial designs rely on heuristic or literature-based shapes—again introducing bias. Accurate evaluation requires EM solvers, which are costly. Surrogate models [14,18] help, but dimensionality and bias persist [19]. More on this topic can be found in [20-24].

ICCS Camera Ready Version 2025
To cite this paper please use the final published version:
DOI: 10.1007/978-3-031-97635-3_47

ML can accelerate designing process by reducing simulation time and predicting antenna behavior. This paper introduces an ML-based framework to evaluate random designs, identify promising geometries for the desired antenna operating range for further optimization, and minimize reliance on EM simulations. It handles designs with 103 parameters, going beyond traditional methods and engineering bias.

The goal is to build an AI-driven system for antenna design and analysis. The system aims to: (1) evaluate random designs without EM simulations, (2) generate designs via generative models, (3) predict antenna responses, and (4) optimize designs via AI. This will enable high-performance, unbiased, fully automated antenna design.

This article addresses the first part of the full system: determining an antenna's operating range from a random design, without EM simulation or expert input. Random generation can yield novel, effective designs. However, most are unsuitable, and filtering them traditionally requires expert knowledge or costly EM simulations. This work proposes a fast ML-based method to estimate the operational range of random designs, enabling quick identification of viable candidates for further optimization.

The contributions are: (1) a methodology for estimating operational range of antennas with random designs via multi-label classification, (2) dataset preparation steps, (3) two neural network architectures—one high-accuracy , one lightweight, (4) training process details to facilitate reproducibility, (5) extensive experimental results.

2 Related Work

In [25,26], ML was applied to optimize antenna design, assuming an initial design based on expert knowledge, with the operational frequency range predetermined. This paper addresses the earlier stage—automating the search for an initial design without expert knowledge, which can later be optimized using methods like those in [25,26].

The work in [27,28] introduced an ML-based antenna synthesis method in three stages: parameter prediction, antenna type classification (e.g., rectangular, horn), and design synthesis. A decision tree classifier was used in [27], while stacking ensemble learning was applied in [28]. The success of neural networks in classification influenced the approach of this paper.

In [29], a survey addressed the regression problem of estimating antennas' frequency responses from designs, using MSE for evaluation. This paper reframes it as a multi-label classification problem, making direct comparison infeasible. In [29], linear regression, support vector regression, polynomial regression, neural networks, and genetic algorithms, were compared demonstrating that neural networks are the most promising approach, which guided the choice of techniques used in this research.

An overview of methods for optimizing antenna designs through regression analysis for various types, including microstrip and patch antennas, was provided in [30]. While direct comparisons with the proposed method are not possible, methods such as support vector machines, Bayesian regularization, and neural networks discussed therein may prove valuable for future research.

Comprehensive reviews of ML methods applied to antenna design and optimization are available in [31,32], offering broad insights into this field.

ICCS Camera Ready Version 2025
To cite this paper please use the final published version:
DOI: 10.1007/978-3-031-97635-3_47

3 Dataset

Planar microstrip antennas are analog devices, and their reflection characteristics over a given frequency range are obtained via EM simulations. An antenna is considered suitable for further optimization if its reflection coefficient is below $\theta_R = -3$dB and its relative bandwidth exceeds $\theta_W = 0.1$ This study introduces a dataset of 106,351 pseudo-random antenna designs with labels indicating whether each sub-band (ten 0.5 GHz sub-bands within 3–8 GHz range) meets both conditions, marking it as suitable for operation and further optimization. Examples are presented in Fig. 1.

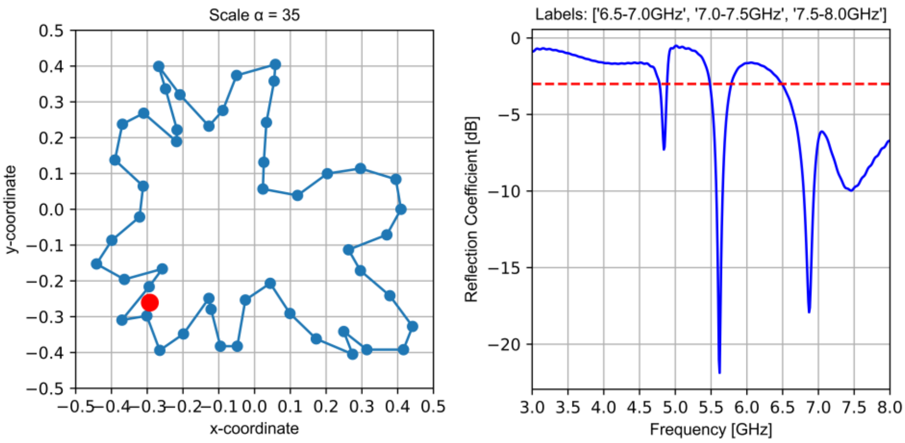

Fig. 1. Example of antenna design (blue – vertices, red – feed point) and antenna response.

A design is a 103-element vector representing an antenna: $\mathbf{D} = [\alpha, q_x, q_y, \mathbf{v}_x, \mathbf{v}_y]$, where $\alpha \in \langle 24,36 \rangle$ is an integer scaling factor, q_x, q_y are feed point coordinates, and $\mathbf{v}_x$, $\mathbf{v}_y$ are 50-element vectors of normalized vertex coordinates ($\in <-1, +1>$). Physical dimensions are given by $\alpha \cdot [\mathbf{v}_x, \mathbf{v}_y]$ and $\alpha \cdot [q_x, q_y]$ in mm. Scaling by α shifts resonance frequencies [18,34]. Designs were generated quasi-randomly [10,11], ensuring no self-intersections and a valid connection between the feed point and the shape.

A label vector is a 10-element vector indicating the antenna's operational range: $\mathbf{B} = [b_g \in \{0,1\}]$, $g = 1,\ldots,10$, where $b_g = 1$ indicates the assignment of the g-th label. The set of labels represents ranges from 3.0 GHz to 8.0 GHz, in 0.5 GHz intervals.

To assign labels to the designs, antenna reflection responses $\mathbf{R}$ [dB] were computed for the frequency range $\mathbf{F}$ [GHz] (see Fig. 1) using EM simulations for 20,000 designs $\mathbf{D}$ with $\alpha = 30$. Simulations were performed using CST Microwave Studio [33], an EM solver based on the Finite Integration Technique [9-11]. To avoid additional costly simulations, responses for other α values were estimated using scaling [18,34]. This can be seen as data augmentation. The computational cost and slight errors in the response amplitude of this interpolation method are negligible. A label vector $\mathbf{B}$ for a given design $\mathbf{D}$ was then assigned using the following algorithm.

1. Compute the set of frequency ranges $\mathbf{Z}$ for which $r_i \leq \theta_R$:

ICCS Camera Ready Version 2025
To cite this paper please use the final published version:
DOI: 10.1007/978-3-031-97635-3_47

$$\mathbf{Z} = \{z_k = [f_{Lk}, f_{Uk}]\},\ k = 1,\ldots,m, \tag{1}$$

$$L_k = \min\{i \mid r_i \leq \theta_R \wedge (i = 1 \vee r_{i\text{-}1} > \theta_R)\},\ i = 1,\ldots,n,\ k = 1,\ldots m, \tag{2}$$

$$U_k = \max\{i \mid r_i \leq \theta_R \wedge (i = n \vee r_{i+1} > \theta_R)\},\ i = 1,\ldots,n,\ k = 1,\ldots m, \tag{3}$$

where f_{Lk} and f_{Uk} are the lower and upper bounds for the k-th frequency range.

2. Compute the set of central frequencies **C** for each range $[f_{Lk}, f_{Uk}]$ as:

$$\mathbf{C} = \{f_{Ck} = (f_{Lk} + f_{Uk}) / 2,\ \forall [f_{Lk}, f_{Uk}] \in \mathbf{Z}\},\ k = 1,\ldots m. \tag{4}$$

3. Compute the set of relative widths **W** for each frequency range in **Z** as:

$$\mathbf{W} = \{w_k = |f_{Uk} - f_{Lk}| / f_{Ck},\ \forall [f_{Lk}, f_{Uk}] \in \mathbf{Z},\ f_{Ck} \in \mathbf{C}\},\ k = 1,\ldots m. \tag{5}$$

4. Define the label set **A** as frequency ranges:

$$\mathbf{A} = \{a_g = [a_{Lg}, a_{Ug}]\},\ g = 1,\ldots,10 = \{[3.0, 3.5],\ldots,[7.5, 8.0]\}\ [\text{GHz}], \tag{6}$$

where a_g is the g-th label, a_{Lg} and a_{Ug} are the bounds for the g-th label.

5. Compute the set of labels $\mathbf{T} \subseteq \mathbf{A}$ that the design must be tagged as:

$$\mathbf{T} = \{a_g \mid w_k \geq \theta_W \wedge ((a_{Lg} < f_{Ck} < a_{Ug}) \vee (f_{Lk} < a_{Lg} \wedge a_{Ug} < f_{Uk}))\}, \tag{7}$$

where $\theta_W \in <0,1>$ is the minimal acceptable relative width threshold.

6. Compute the binary label vector **B** as: $\mathbf{B} = [b_g = \mathbf{1}_\mathbf{T}(a_g)],\ g = 1,\ldots,10$, where $\mathbf{1}_\mathbf{T}(a_g)$ is the indicator function.

An antenna can operate across multiple subranges or have several disjoint ranges; thus, it is a multi-label classification problem, not a multi-class one. Each design in the dataset can be tagged with multiple labels. The dataset is available in [35].

4 Learning Parameters and Model

The proposed method takes a 103-parameter antenna design vector **D** as input and produces a 10-parameter label prediction vector **P** as output. Before entering the model, the design parameters are normalized to the <0,1> range. The model outputs probability scores $\mathbf{S} = [s_g \in <0,1>],\ g = 1,\ldots,10$, where s_g represents the likelihood that the design corresponds to the g-th label. Label predictions **P** are obtained by thresholding **S** at $\theta_P = 0.5$: $\mathbf{P} = [p_g = 1 \text{ if } s_g > \theta_P \text{ else } 0],\ g = 1,\ldots,10$.

The dataset was split into training set (90%) and test set (10%). The training set was used for 10-fold cross-validation. Metrics such as training loss, training accuracy, validation loss, and validation accuracy were recorded, and average values across all folds were computed. The best model, with the lowest validation loss, was selected and tested on the test set, where overall and label-specific accuracy were calculated.

Early stopping, based on validation loss, was applied to prevent overfitting and reduce training time by halting when no improvement was observed. L2 regularization with weight decay was also used to discourage large weights, promoting generalization

ICCS Camera Ready Version 2025
To cite this paper please use the final published version:
DOI: 10.1007/978-3-031-97635-3_47

and simpler models. A learning rate scheduler dynamically adjusted the learning rate to ensure stable convergence and avoid overshooting.

Initial learning parameters were chosen based on the author's experience, and later fine-tuned using grid search. The parameters in Table 1 yielded the best results. The experiments were run on Python 3.11.0 with PyTorch 2.0.1+cu118, utilizing Nvidia GeForce GTX 1080 Ti GPU and CUDA driver 12.2.

Table 1. Learning parameters.

Learning parameter	Value	Learning parameter	Value
Batch size	64	LR scheduler	ReduceLROnPlateau
Loss function	BCE	LR scheduler factor	0.1
Solving algorithm	Adam	LR scheduler patience	5
Initial LR	1e−3	Max epochs	1000
Weight decay	1e−7	Early stopping patience	15

Table 2. Structures of the proposed models.

NN#1 (129,327,626 parameters)	NN#2 (29,814,794 parameters)
Fully Connected (FC) layer, 103 neurons	Fully Connected (FC) layer, 103 neurons
FC, 8192 neurons, LeakyReLU, 0.06 dropout	FC, 4096 neurons, LeakyReLU, 0.06 dropout
FC, 8192 neurons, LeakyReLU, 0.06 dropout	FC, 4096 neurons, LeakyReLU, 0.06 dropout
FC, 4096 neurons, LeakyReLU, 0.06 dropout	FC, 2048 neurons, LeakyReLU, 0.06 dropout
FC, 4096 neurons, LeakyReLU, 0.06 dropout	FC, 2048 neurons, LeakyReLU, 0.06 dropout
FC, 2048 neurons, LeakyReLU, 0.06 dropout	FC, 10 neurons, Sigmoid
FC, 1024 neurons, LeakyReLU, 0.06 dropout	
FC, 512 neurons, LeakyReLU, 0.06 dropout	
FC, 10 neurons, Sigmoid	

Due to the small number of input and output parameters and the multi-label classification nature, a classical neural network (NN) model, specifically a multi-layer perceptron, was chosen. Two models were trained: NN#1 aimed for the highest accuracy, while NN#2 sought similar accuracy with fewer learnable parameters. Various NN architectures were tested, differing in layers, neurons, activations, weights initialization, dropout, and more. The best results were obtained with the structures in Table 2.

The model architecture was designed with input and output layers matching the dataset features. The number of hidden layers and neurons balanced model complexity and performance, as more layers and neurons increase capacity but also the risk of overfitting and computational cost. Various activation functions were tested, with LeakyReLU showing the best performance. Weights were initialized using the Kaiming uniform distribution. Dropout layers were added to reduce overfitting by randomly deactivating neurons during training, promoting diverse feature extraction. The output layer used a sigmoid activation for class probability interpretation.

ICCS Camera Ready Version 2025
To cite this paper please use the final published version:
DOI: 10.1007/978-3-031-97635-3_47

5 Results

Table 3 compares results for models NN#1 and NN#2. Key metrics include label-specific accuracy (per-label performance) and overall accuracy (their average). The table also lists average runtime per sample, covering the entire pipeline: preprocessing, tensor conversion, GPU transfer, classification, and result extraction. For reference, a single EM simulation takes ~60–90 s per design.

NN#1 reached 93.55% overall accuracy, slightly outperforming NN#2 (93.31%). Despite this, NN#2 uses 100 million fewer parameters, offering similar accuracy with lower memory usage and computational cost—beneficial for large-scale use. It should be noted that the models assess whether designs are suitable starting points for optimization. Refining their frequency responses remains outside this work's scope.

Table 3. Results of the experiments.

Model	NN#1	NN#2
Avg. training accuracy	91.76%	87.82%
Avg. validation accuracy	89.54%	85.36%
Training accuracy (best fold)	**97.33%**	**97.56%**
Validation accuracy (best fold)	**93.36%**	**93.04%**
Test label-specific accuracy	[96.91, 94.77, 94.80, 95.51, 95.90, 93.50, 91.18, 91.39, 91.93, 89.65] %	[96.79, 95.04, 95.20, 95.75, 95.83, 93.45, 90.52, 90.39, 91.00, 89.15] %
Test overall accuracy	**93.55%**	**93.31%**
Avg. runtime per sample	0.0026 s	0.0012 s

6 Conclusions

This work introduced a method for estimating operational frequency ranges for planar microstrip antennas with randomly generated designs, bypassing EM simulations and expert input. Framing the task as multi-label classification enables fast, low-cost identification of designs suitable for further optimization.

Future work includes testing on diverse datasets, exploring various random design algorithms, and developing a 2D-CNN classifier due the spatial nature of antenna topologies. Additional plans involve creating a label-to-design generator via an autoencoder with classification support, predicting antenna responses without EM simulations, and building ML-based optimization methods to replace numerical approaches.

Acknowledgments. This work was supported in part by the National Science Centre of Poland (Grant 2021/43/B/ST7/01856).

Disclosure of Interests. The author has no competing interests to declare that are relevant to the content of this article.

References

1. Kouhdaragh, V., Verde, F., Gelli, G., Abouei, J.: On the application of machine learning to the design of UAV-based 5G radio access networks. Electronics 9(4), 689 (2020)
2. Hung, Y.C., Yang, S.H.: Terahertz deep learning computed tomography. In: 2019 44th International Conference on Infrared, Millimeter, and Terahertz Waves (IRMMW-THz), pp. 1–2. IEEE (2019)
3. Shah, S.A., Ahmad, J., Tahir, A., Ahmed, F., Russel, G., Shah, S.Y., Abbasi, Q.H.: Privacy-preserving non-wearable occupancy monitoring system exploiting Wi-Fi imaging for next-generation body centric communication. Micromachines 11(4), 379 (2020)
4. Orabi, M., Khalife, J., Abdallah, A.A., Kassas, Z.M., Saab, S.S.: A machine learning approach for GPS code phase estimation in multipath environments. In: 2020 IEEE/ION Position, Location and Navigation Symposium (PLANS), pp. 1224–1229. IEEE (2020)
5. Lei, L., Lagunas, E., Yuan, Y., Kibria, M.G., Chatzinotas, S., Ottersten, B.: Deep learning for beam hopping in multibeam satellite systems. In: 2020 IEEE 91st Vehicular Technology Conference (VTC2020-Spring), pp. 1–5. IEEE (2020)
6. Wagih, M., Hilton, G.S., Weddell, A.S., Beeby, S.: Millimeter-wave power transmission for compact and large-area wearable IoT devices based on a higher order mode wearable antenna. IEEE IoT J. 9(7), 5229–5239 (2022)
7. Gaya, S., Hamza, A., Sokunbi, O., Sheikh, S.I.M., Attia, H.: Electronically switchable frequency and pattern reconfigurable segmented patch antenna for Internet of Vehicles. IEEE IoT J. 11(10), 17840–17851 (2024)
8. Bod, M., Hassani, H.R., Taheri, M.M.S.: Compact UWB printed slot antenna with extra Bluetooth, GSM, and GPS bands. IEEE Ant. Wireless Prop. Lett. 11, 531–534 (2012)
9. Bekasiewicz, A., Kurgan, P., Kozieł, S.: Numerically Efficient Miniaturization-Oriented Optimization of an Ultra-Wideband Spline-Parameterized Antenna. IEEE Access 10, 21608–21618 (2022)
10. Bekasiewicz, A., Dzwonkowski, M., Dhaene, T., Couckuyt, I.: Specification-Oriented Automatic Design of Topologically Agnostic Antenna Structure. In: Computational Science – ICCS 2024, Lecture Notes in Computer Science, vol. 14834, Springer, 11–18 (2024)
11. Bekasiewicz, A., Askaripour, K.: Performance Comparison of Automatically Generated Topologically Agnostic Patch Antennas. 2024 25th International Microwave and Radar Conference (MIKON), doi: 10.23919/MIKON60251.2024.10633953 (2024)
12. Jacobs, J.P.: Accurate modeling by convolutional neural-network regression of resonant frequencies of dual-band pixelated microstrip antenna. IEEE Ant. Wireless Prop. Lett. 20(12), 2417–2421 (2021)
13. Wu, G.-B., Zeng, Y.-S., Chan, K.F., Chen, B.-J., Qu, S.-W., Chan, C.H.: High-gain filtering reflectarray antenna for millimeter-wave applications. IEEE Trans. Ant. Prop. 68(2), 805–812 (2020)
14. Bekasiewicz, A., Koziel, S., Plotka, P., Zwolski, K.: EM-driven multi-objective optimization of a generic monopole antenna by means of a nested trust-region algorithm. App. Sci. 11(9), art no. 3958 (2021)
15. Whiting, E.B., Campbell, S.D., Mackertich-Sengerdy, G., Werner, D.H.: Dielectric resonator antenna geometry-dependent performance tradeoffs. IEEE Open J. Ant. Prop. 2 (2021)
16. Lizzi, L., Viani, F., Azaro, R., Massa, A.: Optimization of a spline-shaped UWB antenna by PSO. IEEE Ant. Wireless Prop. Lett. 6, 182–185 (2007)
17. Alroughani, H., McNamara, D.A.: The shape synthesis of dielectric resonator antennas. IEEE Trans. Ant. Prop. 68(8), 5766–5777 (2020)

ICCS Camera Ready Version 2025
To cite this paper please use the final published version:
DOI: 10.1007/978-3-031-97635-3_47

18. Koziel, S., Bekasiewicz, A.: Multi-objective design of antennas using surrogate models. World Scientific (2016)
19. Koziel, S., Ogurtsov, S.: Multi-objective design of antennas using variable-fidelity simulations and surrogate models. IEEE Trans. Ant. Prop. 61(12), 5931–5939 (2013)
20. Koziel, S., Bekasiewicz, A.: Fast multi-objective design optimization of microwave and antenna structures using data-driven surrogates and domain segmentation. Engineering Computations 37, 735–788 (2019)
21. Koziel, S., Bekasiewicz, A.: Domain segmentation for low-cost surrogate-assisted multi-objective design optimization of antennas. IET Microwaves, Antennas & Propagation 12(10), 1728–1735 (2018)
22. Koziel, S., Bekasiewicz, A.: Comprehensive comparison of compact UWB antenna performance by means of multiobjective optimization. IEEE Transactions on Antennas and Propagation 65(7), 3427–3436 (2017)
23. Koziel, S., Bekasiewicz, A.: Rapid simulation-driven multiobjective design optimization of decomposable compact microwave passives. IEEE Transactions on Microwave Theory and Techniques 64(8), 2454–2461 (2016)
24. Koziel, S., Bekasiewicz, A.: Multi-objective optimization of expensive electromagnetic simulation models. Applied Soft Computing 47, 332–342 (2016)
25. Gampala, G., Reddy, C.J.: Fast and Intelligent Antenna Design Optimization using Machine Learning. 2020 International Applied Computational Electromagnetics Society Symposium (ACES), doi: 10.23919/ACES49320.2020.9196193 (2020)
26. Wu, Q., Chen, W., Yu, C., Wang, H., Hong, W.: Machine-Learning-Assisted Optimization for Antenna Geometry Design. IEEE Trans. Antennas Propag. 72(3), doi: 10.1109/TAP.2023.3346493 (2024)
27. Ramasamy, R., Bennet, M.A.: An Efficient Antenna Parameters Estimation Using Machine Learning Algorithms. Prog. Electromagn. Res. C 130, 169–181 (2023), doi: 10.2528/PIERC22121004
28. Shi, D., Lian, C., Cui, K., Chen, Y., Liu, X.: An Intelligent Antenna Synthesis Method Based on Machine Learning. IEEE Trans. Antennas Propag. 70(7), doi: 10.1109/TAP.2022.3182693 (2022)
29. ElAbbasi, M.K., Madi, M., Kabalan, K.Y.: Optimization of Antenna Dimensions for Improved Frequency Response using Machine Learning: A Survey. 2024 6th Int. Conf. on Commun., Signal Processing, and their Appl. (ICCSPA) (2024)
30. El Misilmani, H.M., Naous, T.: Machine Learning in Antenna Design: An Overview on Machine Learning Concept and Algorithms. 2019 International Conference on High Performance Computing & Simulation (HPCS) (2019)
31. Khan, M.M., Hossain, S., Mozumdar, P., Akter, S., Ashique, R.H.: A review on machine learning and deep learning for various antenna design applications. Heliyon 8(4), e09317 (2022), doi: 10.1016/j.heliyon.2022.e09317
32. Sarker, N., Podder, P., Mondal, M.R.H., Shafin, S.S., Kamruzzaman, J.: Applications of Machine Learning and Deep Learning in Antenna Design, Optimization, and Selection: A Review. IEEE Access 11, doi: 10.1109/ACCESS.2023.3317371 (2023)
33. CST Microwave Studio, Dassault Systems, 10 rue Marcel Dassault, CS 40501, Vélizy-Villacoublay Cedex, France (2015)
34. Koziel, S., Yang, X.S. (Eds.): Computational Optimization, Methods and Algorithms. Studies in Computational Intelligence, Springer-Verlag (2011)
35. Czaplewski, B.: 1Ddesign-to-label-1.8.3 - Antenna Designs with Operating Frequency Range Labels (1.8.3) [Data set]. Gdańsk University of Technology, Faculty of Electronics, Telecommunications and Informatics (2025). https://doi.org/10.5281/zenodo.14982975

ICCS Camera Ready Version 2025
To cite this paper please use the final published version:
DOI: 10.1007/978-3-031-97635-3_47